Biosensors and Bioelectronics 137 (2019) 25–32

Contents lists available at ScienceDirect

Biosensors and Bioelectronics

journal homepage: www.elsevier.com/locate/bios

Hydrogel optical fibers for continuous glucose monitoring

Mohamed Elsherif[a,b,**], Muhammad Umair Hassan[c], Ali K. Yetisen[d], Haider Butt[e,*]

[a] School of Engineering, University of Birmingham, Birmingham, B15 2TT, UK
[b] Department of Experimental Nuclear Physics, Nuclear Research Center, Egyptian Atomic Energy Authority, Egypt
[c] Optoelectronics Research Lab, COMSATS University Islamabad, Park Road, Islamabad, 45550, Pakistan
[d] Department of Chemical Engineering, Imperial College London, London, SW7 2AZ, UK
[e] Department of Mechanical Engineering, Khalifa University, Abu Dhabi, 127788, UAE

ARTICLE INFO

Keywords:
Photonics
Fiber optics
Sensors
Continuous glucose monitoring
Boronic acids

ABSTRACT

Continuous glucose monitoring facilitates the stringent control of blood glucose concentration in diabetic and intensive care patients. Optical fibers have emerged as an attractive platform; however, their practical applications are hindered due to lack of biocompatible fiber materials, complex and non-practical readout approaches, slow response, and time-consuming fabrication processes. Here, we demonstrate the quantification of glucose by smartphone-integrated fiber optics that overcomes existing technical limitations. Simultaneously, a glucose-responsive hydrogel was imprinted with an asymmetric microlens array and was attached to a multimode silica fiber's tip during photopolymerization, and subsequent interrogated for glucose sensing under physiological conditions. A smartphone and an optical power meter were employed to record the output signals. The functionalized fiber showed a high sensitivity (2.6 μW mM^{-1}), rapid response, and a high glucose selectivity in the physiological glucose range. In addition, the fiber attained the glucose complexation equilibrium within 15 min. The lactate interference was also examined and it was found minimal ~0.1% in the physiological range. A biocompatible hydrogel made of polyethylene glycol diacrylate was utilized to fabricate a flexible hydrogel fiber to replace the silica fiber, and the fiber's tip was functionalized with the glucose-sensitive hydrogel during the ultraviolet light curing process. The biocompatible fiber was quickly fabricated by the molding, the readout approach was facile and practical, and the response to glucose was comparable to the functionalized silica fiber. The fabricated optical fiber sensors may have applications in wearable and implantable point-of-care and intensive-care continuous monitoring systems.

1. Introduction

Stringent control of blood glucose concentration is essential in preventing hyper/hypoglycemia that may lead to serious diabetic complications including diabetic retinopathy, foot ulcers, diabetic nephropathy, and atherosclerosis (The Action to Control Cardiovascular Risk in Diabetes Follow-On Eye Study et al., 2016; Skyler et al., 2009; Srinivasan et al., 2015; Crofford et al., 1987). Hyperglycemia may be found in intensive-care patients even in those without a clinical history of diabetes such as patients of high-degree burns, trauma, hypoxia, sepsis, and shock, where the stress of acute illness induces glucose production, insulin resistance, and relative insulin deficiency (Thompson et al., 2005; Van Den Berghe et al., 2001; Williams et al., 2002; Van den Berghe, 2002; Umpierrez et al., 2002; Montori et al., 2002; Finney et al., 2003; Kondepati and Heise, 2007). A strict blood glucose management for the patients with acute illness or in the intensive care unit (ICU) decreases the risk of morbidity and mortality (Finney et al., 2003; Kondepati and Heise, 2007; Haga et al., 2011; Doran et al., 2004). A recent economic analysis of conventional and intensive glucose concentration management in ICUs has demonstrated a significant reduction in the overall medical care costs (Rapsang and Shyam, 2014; Krinsley and Jones, 2006a; Van den Berghe et al., 2006). The strict control of glucose concentration for acute illness saved around $1580 per adult patient resulting from the shorter ICU period and hospitalization, curtailment of the ventilator-dependent days, and cutting down the laboratory cost (Rapsang and Shyam, 2014; Krinsley and Jones, 2006b). Therefore, tight control of glycemia provides favorable results in terms of clinical outcome and cost-effectiveness.

Commercial glucose monitoring systems are based on finger prick testing that should be carried out up to 3–5 times a day (Kondepati and

* Corresponding author.
** Corresponding author. School of Engineering, University of Birmingham, Birmingham, B15 2TT, UK.
E-mail addresses: m_elshereif@aucegypt.edu (M. Elsherif), haider.butt@ku.ac.ae (H. Butt).

https://doi.org/10.1016/j.bios.2019.05.002
Received 4 April 2019; Accepted 1 May 2019
Available online 02 May 2019
0956-5663/

Heise, 2007). However, the finger prick testing may not be accurate as compared to blood venous samples, for example, the postprandial glucose concentration in capillary blood can be 35% higher than that of in venous blood (Yang et al., 2012). Therefore, an alternative non-invasive or minimally-invasive system would eliminate the inconvenience of the frequent pain and aids to the strict control of the glucose concentration in the blood. To address this clinical need, implantable electrochemical sensors have been developed for short-term continuous glucose monitoring. However, these sensors have several drawbacks: (i) they are unstable *in vivo* due to the enzymatic reaction leading to the signal drift, (ii) their activity is oxygen dependent, (iii) they are inaccurate in low glucose concentrations, and (iv) they cannot be used for long-term continuous glucose monitoring (Heo et al., 2011). Recently, minimally-invasive contact lenses sensors were introduced for quantifying glucose concentration in tears; however, the concentration of glucose in tears may not accurately correlate with blood glucose (Elsherif et al., 2018a, 2018b).

Fiber optic probes as minimally-invasive sensors have been developed for *in vivo* glucose monitoring to provide continuous quantitative analysis (Yang et al., 2012; Yetisen et al., 2017). For instance, the surface plasmon resonance probes have been emerged as a strong candidate; however, they suffer from complex fabrication process, and convoluted readout process (Li et al., 2015a, 2015b; Cao et al., 2018; Srivastava et al., 2012; Singh and Gupta, 2013; Lin and Chung, 2009). Also, interferometric fiber probes have been developed for *in vivo* glucose sensing (Tierney et al., 2009). The readout of that probe was complicated and the output signals were processed to detect the volumetric response attached to the fiber's tip. In addition, the silica fiber probe is not compatible with biological systems for implementation *in vivo* as it causes immune response resulting in inflammation and discomfort of patients (Ruckh and Clark, 2013; Heller and Feldman, 2008; Vaddiraju et al., 2010).

Hydrogel fibers were introduced as a promising technology for *in vivo* glucose sensing due to their biocompatibility and capability to incorporate functional groups (Choi et al., 2013). Functionalizing the hydrogel fiber with glucose-recognition motif such as phenylboronic acid (PBA) derivatives modulates the optical properties of the fiber due to glucose-boron complexation. For instance, a hydrogel fiber probe based on fluorescence has been reported for quantitative glucose measurements, in which the glucose recognition motif, diboronic acid, and the fluorescent dye (anthracene acid) were incorporated (Heo et al., 2011). Despite the rapid response of the fluorescent fiber probe, it suffered from photobleaching of the fluorophore, it was not applicable to individuals with skin pigmentation, and the output signal was affected by epidermal thickness. Recently, polyacrylamide optical fibers were functionalized with 3-(acrylamido)phenylboronic acid (Yetisen et al., 2017). The fiber diameter increased in response to glucose leading to a change in the transmitted light intensity. However, the fiber required long time to reach equilibrium of glucose complexation, which is not practical for *in vivo* glucose detection.

Here, we developed optical fiber probe for continuous glucose monitoring in physiological conditions. The glucose recognition agent (3-(acrylamido)-phenylboronic acid) was crosslinked with acrylamide to create glucose-responsive hydrogel and an asymmetric microlens array (light diffusing microstructures, LDMs) was imprinted on the hydrogel. The glucose-responsive hydrogel was chemically attached to the tip of a silica multimode fiber during the photopolymerization process. The functionalized fiber was interrogated for glucose quantification in the transmission and reflection configurations. Upon glucose complexation with the boronic acid groups immobilized in the hydrogel matrix, the hydrogel attached the fiber shifted volumetrically, altering the curvatures of the imprinted asymmetric microlens array. Accordingly, the transmitted and the reflected optical powers of the functionalized fiber were measured by an optical powermeter or a smartphone. In addition, the hydrogel sensor was attached to the tip of a biocompatible hydrogel fiber. The biocompatible functionalized fiber was flexible and offered the convenience to be potentially implemented in biological tissues. The proposed glucose-responsive probe has additional advantages over the previously developed fiber probes, such as (i) easy readout process as it is compatible with smartphones and no output signal processing is required, (ii) rapid response (30 s) and short equilibrium time (15 min), and (iii) low-cost, glucose-selective, and plug-and-play technology.

2. Materials and methods

2.1. Materials

Polyethylene glycol diacrylate (PEGDA) (mw: 700 Da), acrylamide (AM) (98%), 3-(acrylamido)-phenylboronic acid (3-APBA) (98%), sodium L-lactate, *N,N′*-methylenebisacrylamide (99%), D-(+) glucose (99.5%), 2,2-dimethoxy-2-phenylacetophenone (DMPA) (99%), 2-hdroxy-2-methylpropiophenone (2-HMP) (97%), phosphate buffered saline tablets (PBS), dimethyl sulfoxide (DMSO) (99.9%), sodium phosphate monobasic (NaH_2PO_4), and sodium phosphate dibasic (NaH_2PO_4) were purchased from Sigma Aldrich and used without further purification.

2.2. Fabrication of the hydrogel sensor constrained on a glass slide

The precursor solution consisted of acrylamide (78.5 mol %), *N*, *N′*-methylenebisacrylamide (1.5 mol %), and 3-APBA (20 mol %) was mixed with DMPA (2% wt/vol) in DMSO and the monomer dilution was 1:2 wt/vol. The monomer solution (100 µl) was drop-cast on the asymmetric microlens array surface (Thorlabs), and subsequently, was covered with a salinized glass piece, and was polymerized by UV lamp (365 nm) for 5 min. The polymerized sensor was washed with DI water/ethanol (1:1 v/v) and preserved in PBS solution at pH 7.4.

2.3. Functionalization of the silica and the hydrogel fibers

To functionalize the optical fiber with the glucose responsive hydrogel, the fiber's tip was silanized and dipped in the glucose-sensitive solution (10 µl) that was drop-cast on the asymmetric microlens array surface (AMLA) and was exposed to the UV light for 5 min. The functionalized fiber was preserved in the PBS solution at pH 7.4.

2.4. Fabrication of the biocompatible optical fiber

PEGDA monomer was mixed with 2-hydroxy-2-methylpropiophenone (2-HMP) (5 vol %) in DI water. The dilution of PEGDA in DI water was varied from 5 to 90 vol%. The prepared solution (200 µl) was injected into a polyvinyl chloride tube with an inner diameter of 1 mm and the tube was exposed to UV light (365 nm) for 30 min. The optical fiber was extracted from the tube by applying water pressure using a syringe. The optical fiber was washed with a mixture of ethanol and DI water (1:1, v/v).

3. Results and discussion

The glucose-responsive hydrogel was fabricated, functionalized with the 3-APBA, and stamped with asymmetric microlens arrays during the photopolymerization (Fig. 1a). Distribution of the microlens array and the optical microscope image are displayed in the supplementary file, Fig. 1. The stamped hydrogel sensor was attached to a commercial multimode silica fiber and an in-house made biocompatible fiber during the polymerization process (Fig. 1b and c). Fabrication of the biocompatible fibers is shown in Fig. 1d. The immobilized 3-APBA in the hydrogel matrix of the sensor has a high affinity to glucose molecules forming anionic boronate due to 1:1 complexation in the hydrogel network, increasing the osmotic Donnan pressure, and accordingly causing a volumetric shift (supplementary file, Fig. 2).

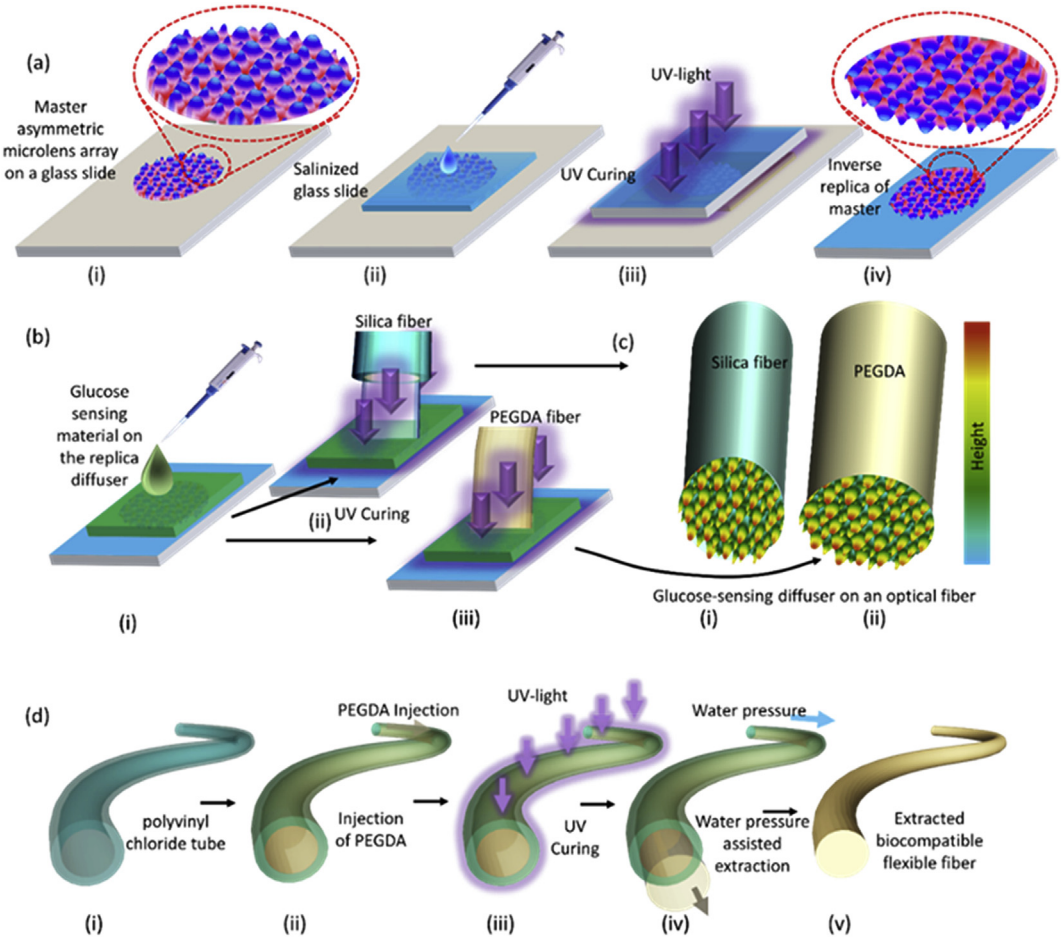

Fig. 1. Fabrication of the glucose-responsive hydrogel, functionalizing the fibers, and fabrication of the hydrogel fiber. (a) Schematic show the procedures of preparing the glass constrained glucose-responsive hydrogel stamped with asymmetric microlens array. (b–c) The functionalization process of the silica and the hydrogel fibers. (d) The fabrication process for the biocompatible hydrogel fiber.

(Hisamitsu et al., 1997) The volumetric shift of the hydrogel modified the curvature of the asymmetric microlens array stamped on the hydrogel's surface leading to change the focal lenses of the microlenses, and consequently the maximum transmitted/reflected power that was correlated to the measured glucose concentration.

The prepared hydrogel sensor constrained on a glass substrate and stamped with an asymmetric microlens array was examined in various glucose concentrations (0–50 mM). The sensor was equilibrated in PBS solution (pH 7.4, ionic strength 150 mM, 24 °C) for 2 h before testing. A stock glucose solution (100 mM) was prepared in PBS buffer of pH 7.4 and diluted using the PBS solution to prepare the required glucose concentrations. The sensor was submerged in glucose-free PBS buffer solution (1 ml) and illuminated with a green laser (532 nm) and the spatial profile of the transmitted power (SP_t) was recorded as a reference (Fig. 2a). The glucose-free PBS buffer was replaced with a buffered glucose solution (1 ml, 5 mM), and the SPTP was recorded after 15 min. The low glucose concentration (5 mM) was replaced with a higher concentration (10 mM) and the reading was recorded after 15 min, and this protocol was repeated until reaching 50 mM. The recorded SP_t for the sensor in various glucose concentrations presented Gaussian shape profiles and the forward scattering angles decreased with increasing glucose concentrations. The diffused light formed a spot having smaller diameter on the screen, increasing the maximum optical transmitted power (P_t) with glucose concentration (Fig. 2b). The P_t readings as a practical readout method were utilized to monitor the glucose concentrations. The sensor's response saturated with increasing glucose concentration; however, it presented a linear response within the range of 0–20 mM, which had a correlation coefficient, R^2 of 0.99 (Fig. 2c). The P_t increased from 79.4 to 86.7 μW when glucose concentration increased from 0 to 10 mM, and reached 99 μW when glucose concentration increased to 50 mM. To confirm the working principle, the surface morphology of the hydrogel sensor was investigated under the optical microscope while the sensor was submerged in glucose-free PBS buffer and PBS buffer of 50 mM glucose concentration. Upon glucose-boron complexation, the sensor swelled in z-direction only as it was constrained on the glass slide. Consequently, the curvature of the imprinted microlenses became flatter (supplementary file, Fig. 3a and b). The surface profile analysis showed that the depth of the microlens array was higher under glucose-free condition as compared to the surface's depth in glucose condition (Supplementary file, Fig. 3c). Again, the hydrogel sensor was examined for glucose sensing, but in this test, the sensor was illuminated by a broadband white light beam and the output signals, the maxima transmitted illuminance (L_t), were measured by a smartphone (Fig. 2d). Thirdly, the sensor was interrogated in the reflection configuration as the sensor was illuminated by a monochromatic light (532 nm) at an incident angle of 45° and the maximum reflected powers (P_r) of the diffused beam were collected using an optical power meter (Fig. 2d). The ambient light sensor of a smartphone was utilized to record the output signals to demonstrate the compatibility and the simplicity of the readout process. The readout for the glucose-free buffer was 60 lux and jumped up to 69 upon increasing glucose concentrating from 0 to 20 mM and reached to 75 lux at 50 mM (Fig. 2e). The relationship of the glucose concentration against the sensor's output signal was consistent with the experiment carried out

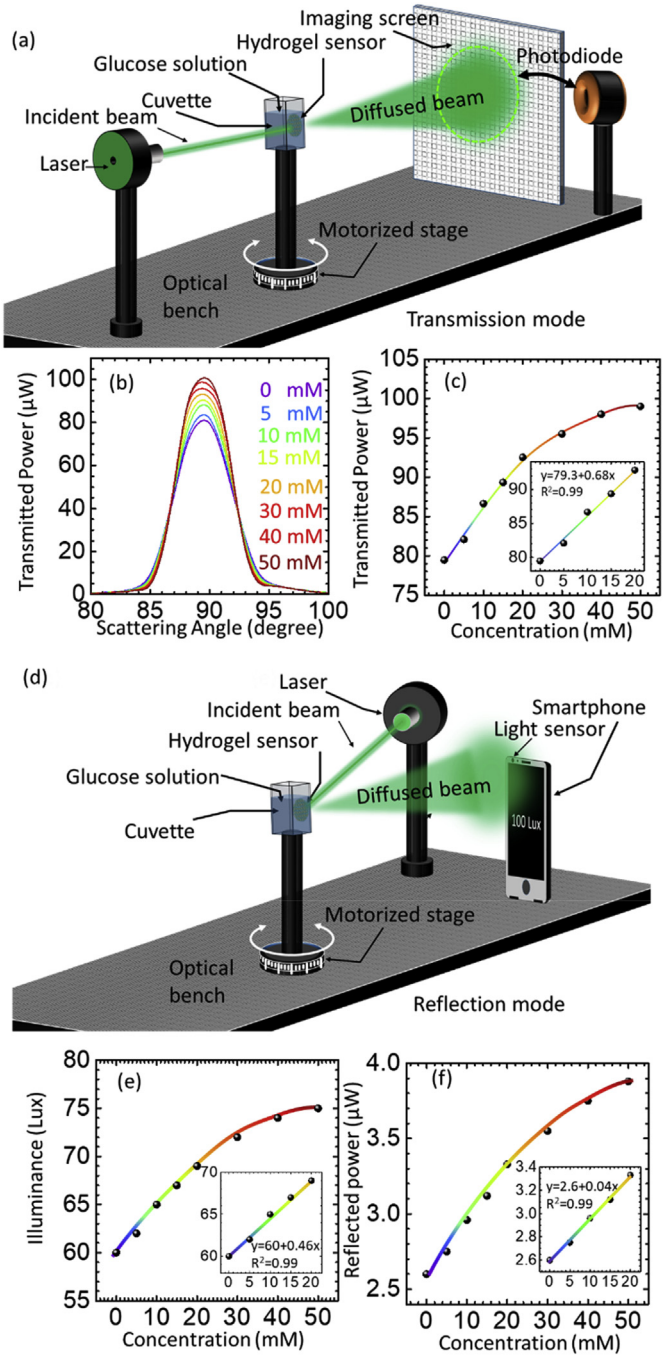

Fig. 2. Quantification of glucose concentration by the hydrogel sensor. (a) Schematic of the setup for recording glucose concentrations in the transmission mode. (b) The profile of the optical transmitted power passing through the sensor against glucose concentrations when the sensor was illuminated by a green laser (532 nm). (c) P_t of the sensor at various glucose concentrations (0–50 mM). The inset shows the glucose range of 0–20 mM. (d) Schematic of the setup utilized for interrogating the glucose sensor in the reflection mode. (e) The maximum transmitted illuminance (L_t) of the sensor *versus* glucose concentrations while the sensor was illuminated by the broadband white light beam, and the illuminance was recorded by an ambient light sensor of a smartphone. (f) The P_r of the hydrogel sensor for various glucose concentrations captured in reflection mode. The inset shows the glucose concentrations range of 0–20 mM. (For interpretation of the references to colour in this figure legend, the reader is referred to the Web version of this article.)

using the monochromatic light and the optical power meter (Fig. 2c). The sensor's response was linear for glucose concentration range of 0–20 mM with a correlation coefficient, R^2 of 0.99 and saturated at high glucose concentrations. The hydrogel sensor consistently detected glucose concentrations whether it was illuminated by a monochromatic light or a broadband white light and this is due to the ability of the microlenses array to control the beam shape of the monochromatic and white light. In reflection configuration, the P_r increased with glucose concentration because of the positive volumetric shift of the hydrogel sensor, decreasing the curvature of the microlenses and consequently the light diffusion efficiency of the sensor (Fig. 2f). The sensor behavior was consistent with the experiments that were carried out in the transmission mode (Fig. 2c). The P_t increased from 2.6 μW to 3.33 μW upon increasing glucose concentration to 20 mM and reached 3.88 μW at 50 mM (Fig. 2f). The sensor's output signals saturated at a high glucose concentration (30 mM) and the correlation coefficient had a linear relationship (R^2 = 0.99) for glucose concentration within the range 0–20 mM.

For *in vivo* or remote glucose sensing applications, the hydrogel sensor was attached to the tip of a multimode silica fiber having a diameter of 500 μm. The silica fiber with the functionalized tip was utilized for glucose detection *in vitro* in both transmission and reflection configurations. In the transmission mode, the fiber was coupled with a monochromatic light source (532 nm) and the output signals (P_t) were recorded by either an optical power meter or a smartphone (Fig. 3a). Optical microscopy images of the fiber's cross-section and photos of the functionalized fiber illuminated by different monochromatic light sources (Fig. 3b–d). The fabrication process of the functionalized silica fiber including preparing the hydrogel matrix, functionalizing the hydrogel with 3-APBA, imprinting the asymmetric microlens array and attaching the hydrogel sensor to the fiber's tip was carried out in one stage lasting 5 min (Fig. 1b). This facile and rapid fabrication approach is one of the great advantages of the developed sensor as compared to other fiber optic probes such as fluorescent and SPR based probes. For instance, the preparation of the fluorescent glucose sensor requires multiple reaction stages and time-consuming synthesis and purification (Veetil et al., 2010). On the other side, the fabrication of the SPR fiber probes is complicated and requires many steps: pretreatment of the optical fiber, decladding, depositing the metal thin layer, immobilizing the glucose sensitive layer (Li et al., 2015b; Srivastava et al., 2012; Singh and Gupta, 2013).

The fiber probe was tested in glucose concentration range of 0–50 mM and the P_t for each concentration over time were recorded at 24 °C (Fig. 3e). When glucose concentration was increased, the fiber's output signal (P_t) increased, showing a linear trend with a correlation coefficient R^2 of 0.99 for glucose concentration range of 5–20 mM. Upon increasing glucose concentration from 0 to 20 mM, P_t surged 48 μW, from 602 to 650 μW (Fig. 3f). For high glucose concentrations from 20 to 50 mM, the P_t increased 30 μW, indicating declined sensitivity. The 8.3% when glucose concentration increased from 0 to 20 mM as compared to 7% change over the glucose concentration range of 0–100 mM for previously developed fiber probes (Yetisen et al., 2017). The optical fiber was coupled with a green laser and was re-interrogated for glucose sensing; however, in this test, a smartphone was employed to measure the output signals. The maximum transmitted illuminance (L_t) increased by 69 Lux, from 929 to 998 Lux with increasing glucose concentration from 0 to 20 mM; however, the growth of the output signal was 49 Lux when glucose concentration increased from 20 to 50 mM (Fig. 3g). The trend of the recorded L_t against the glucose concentrations was comparable to results recorded by the optical power meter. The fiber probe's response was linear for glucose concentration range of 5–20 mM with a correlation coefficient R^2 of 0.99 and the sensitivity declined at high concentrations as the sensor saturated. To test the feasibility of utilizing the broadband white light for sensing as it is safer than laser for human body implantation sensing, the functionalized fiber was coupled with a broadband white light

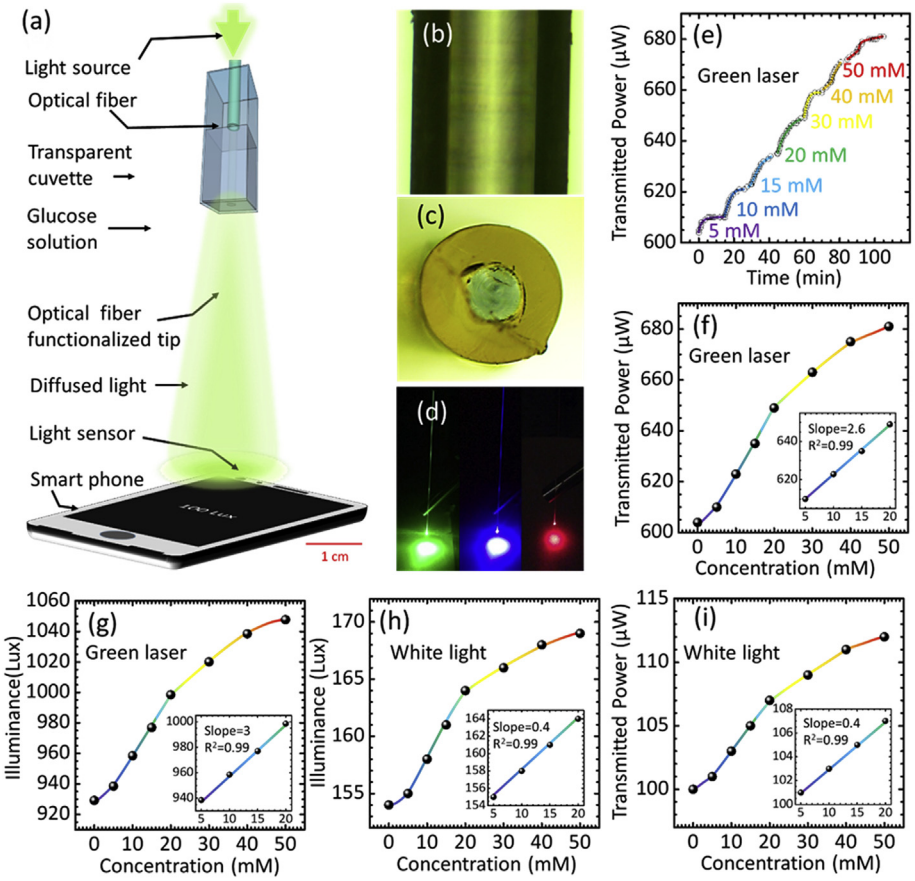

Fig. 3. Detection of glucose with functionalized silica fiber in transmission mode. (a) Schematic of the setup utilized to test the functionalized fiber in the transmission mode. (b–c) Optical microscopy images of the silica multimode fiber. (d) Photographs of the functionalized silica fiber coupled with blue, green, and red lasers. (e) The maximum optical transmitted power (P_t) of the functionalized fiber submerged in various glucose concentrations over time. (f) The P_t of the fiber against glucose concentrations (0–50 mM), while the fiber was coupled with a green laser and the readout was recorded by a power meter. The inset shows measurements for the glucose range of 5–20 m. (g) The L_t of the fiber *versus* glucose concentrations where the fiber was coupled with a green laser pointer and the readouts were captured by an ambient light sensor of a smartphone. The inset shows the glucose concentration range of 5–20 mM. (h) The L_t of the optical fiber versus glucose concentrations while the fiber was coupled with a broadband white light source and the output signals were captured by an ambient light sensor of a smartphone. The inset shows the glucose concentration range of 5–20 mM. (i) The P_t of the optical fiber *versus* glucose concentrations where the fiber was coupled with a broadband white light source and the output signals were recorded by an optical power meter. The inset shows the glucose concentration range of 5–20 mM. (For interpretation of the references to colour in this figure legend, the reader is referred to the Web version of this article.)

source and re-examined for glucose concentrations within the range of 0–50 mM and the readout was collected by a smartphone and an optical power meter (Fig. 3h and i). The trends of the output signals from the fiber probe immersed in various glucose concentrations were comparable whether the output signals were recorded by the smartphone or the optical power meter. The probe's response decreased at high concentrations and below 30 mM, the response was linear with a correlation sensor's saturation at high glucose concentrations might be attributed to the limited available boronate binding sites and the reduced elasticity of the hydrogel matrix that competed against the volumetric swelling process (Elsherif et al., 2018a). The fiber probe interrogation results matched with the previous experiments carried out when the hydrogel glucose sensor was constrained on a glass substrate. The fiber sensitivity was 2.6 μW mM^{-1} in the most significant glucose concentration range (5–20 mM), calculated using the slope of the linear fit. The output signal of the optical fiber shifted by coefficient R^2 of 0.99. Advantageously, the probe's response to glucose concentrations was similar whether the coupled light source was a broadband white light or a monochromatic light source, and the smartphone was successfully employed for readouts and showed a reliable response. The readout methodology was simple and low cost whether the output signal was recorded by a power meter or a smartphone and this one of the main advantages of the developed fiber probe as compared to the previous reposted glucose probes (Yetisen et al., 2017; Li et al., 2015a; Tierney et al., 2009). For instance, interferometric, fluorescent, and SPR fiber probes require processing of the output signal and high-cost instruments such as spectrophotometers and fluorometers for readout (Li et al., 2015b; Tierney et al., 2009).

The functionalized silica fiber was also tested for glucose sensing within the concentration range of 0–50 mM, but this time in the reflection configuration, which is the desired mode for *in vivo* glucose sensing. In the reflection configuration, a three terminal coupler 2 × 1 was utilized to connect the fiber with the white light source and the optical power meter (Fig. 4a). The fiber was submerged in the glucose solution (1 ml) and the optical reflected power (P_r) was recorded by the power meter. Upon swelling of the hydrogel sensor fixed at the fiber's tip, the P_r guided in the optical fiber increased (Fig. 4b). In the reflection mode, the behavior of the output signal against glucose concentrations was comparable to the measurements in the transmission mode as the fiber response was linear within the concentration range of 0–20 mM with a correlation coefficient R^2 of 0.99, and the sensitivity decreased significantly above 20 mM. The optical reflected power was 318 nW for the glucose-free PBS buffer and increased to 338 nW at 20 mM concentration with a sensitivity of 1 nW mM^{-1} in this glucose range. For the high glucose concentration range of 20–50 mM, the output signal recorded an increment of 13 nW.

The swelling dynamics of the fiber probe was studied at a constant glucose concentration (10 mM) as the P_t was recorded over time. Upon exposure of the fiber to the glucose solution, the binding equilibrium (glucose-boron complexation) saturated within 15 min and the response time was 30 s (Fig. 4c). This equilibrium time was one-third of the response times reported in previous studies, where the saturation time for the 3-APBA-modified optical fiber was 45 min (Yetisen et al., 2017). For the diabetic patients, the readout rate required for monitoring glucose concentration is 0.078 mM·min^{-1}, and the proposed probe provided a readout rate of 0.66 mM min^{-1}, which is 8-fold higher than the required speed (Yetisen et al., 2017). The stability and reusability of the functionalized silica fiber were investigated by detecting the response of the fiber in four complete and continuous cycles (Fig. 4d). The probe's response for 10 mM glucose concentration was monitored for 15 min, followed by a reset using an acetate buffer (pH 4.6) for ~10 s, and maintained in PBS for 15 min buffer before commencing the next cycle. When the fiber was immersed in buffer at pH 4.6, the hydrogel attached sensor shrank due to the decrease in the pH below the

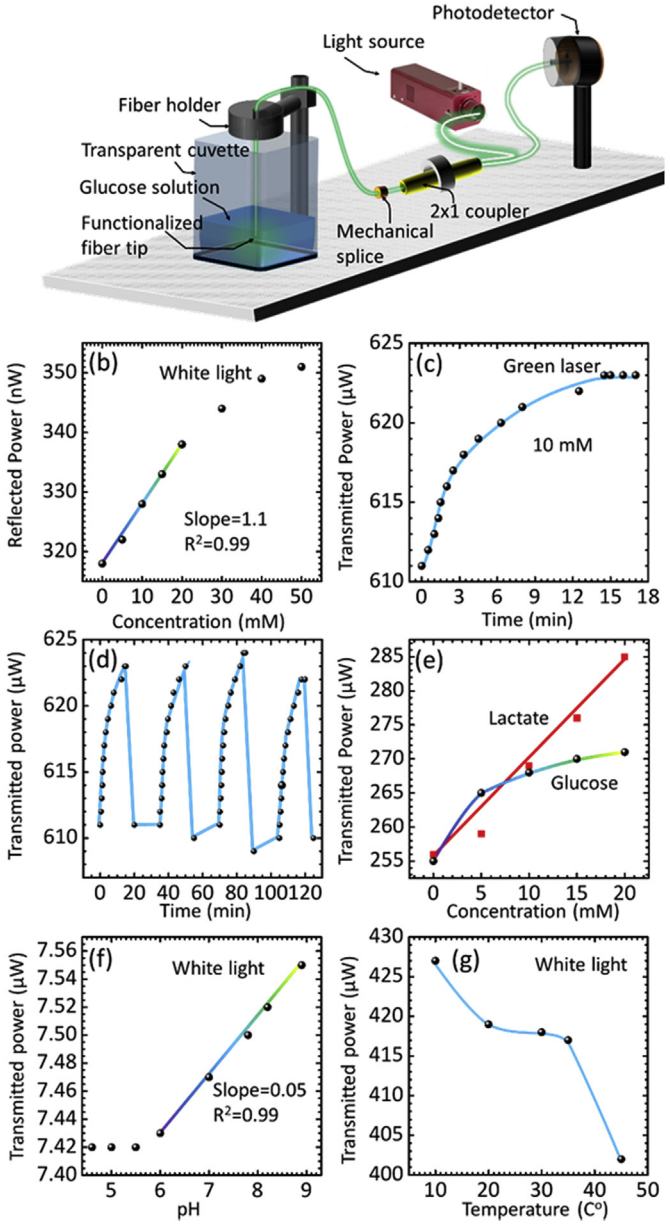

Fig. 4. The functionalized silica fiber used for glucose sensing in reflection mode. (a) Schematic of the setup utilized for interrogating the functionalized fiber in the reflection configuration. (b) The optical reflected power *versus* the glucose concentrations while the fiber coupled with a white light source and the output signal was captured by an optical power meter. (c) The maximum transmitted power of the functionalized fiber over time at 10 mM glucose concentration. (d) The fiber's output signal *versus* time at a glucose concentration of 10 mM for four cyles as the green laser laser pointer coupled with the fiber and the readings were recorded in transmission mode, the fiber was reset in acetate buffer (pH 4.6), and the transmitted power baseline was 611 ± 1 μW and increased to 623 ± 1 μW. (e) The lactate and glucose concentrations *versus* the P_t at human body temperature, 37 °C, the test was carried out in the transmission mode. (f) The solution's pH against the fiber's output signal recorded in the transmission mode. (g) The solution' temperature *versus* the fiber's output signals, the test was carried out in the transmission mode. (For interpretation of the references to colour in this figure legend, the reader is referred to the Web version of this article.)

apparent pK_a value of the glucose-responsive hydrogel as the charged tetrahedral state of the 3-APBA transformed to uncharged trigonal planar form releasing the bound glucose molecules (Yetisen et al., 2017). Upon immersing the functionalized tip into the PBS buffer of pH 7.4, the attached hydrogel returned to it is original volume, and consequently the asymmetric microlens array was reset to its original geometry. These results are significant as the functionalized fiber exhibited reusability with limited hysteresis and had comparable sensitivity for each cycle. The boronic acids bind to *cis*-diol containing molecules and α-hydroxy acids. Fructose and galactose are monosaccharides present in human blood at low concentrations (< 0.1 mM)_ (James et al., 1994; Kabilan et al., 2005). In addition, there are many other sugars in blood in the form of glycoproteins and macromolecular carbohydrates; however, they are not expected to significantly interfere with the probe's response as they may not diffuse into the hydrogel matrix and bind to PBA groups because of their large molecular sizes (Kabilan et al., 2005). Thus, the glucose selectivity during *in vivo* sensing was expected to be minimal; however, lactate is present in blood at a concentration of 0.36–0.75 mM in healthy adults and has a high affinity to bind with phenylboronic acid by its *α*-hydroxy group (Yetisen et al., 2017). Hence, the potential interference of lactate on the probe's response was interrogated (Fig. 4e). The lactate solutions were prepared in PBS buffer (pH 7.4) and the probe's response for lactate and glucose were recorded separately at human body temperature (37 °C) to determine the potential interference of lactate under the physiological conditions. The recorded output signals (P_t) of the fiber probe shifted significantly at high lactate concentrations, but subtly any response was recorded at low lactate concentrations (1.0 mM). On the contrary, the output signal of the fiber considerably shifted at low glucose concentrations within the physiological range (4.0–8.0 mM) and the fiber response saturated at higher concentrations (Boeckxstaens et al., 1997; Thomé-Duret et al., 1996). At a lactate concentration of 5.0 mM, the output signal increased by 1.2% over 15 min as compared to 4% increase for the same concentration of glucose in the same interval. Therefore, the interference of the lactate according to its concentrations in blood would be 0.08%–0.17%. However, the small molecular weight (Mw: 90 g mol^{-1}) of lactate molecule accelerated its diffusion into the hydrogel matrix and its high affinity to bind with the pendant phenylboronic acid, it has a limited potential interference in the fiber's response (Yetisen et al., 2017; Bajgrowicz-Cieslak et al., 2017).

The effect of pH on the probe's response was examined as the probe was submerged in various pH solutions of same ionic strength (150 mM) at 24 °C and the P_t was recorded (Fig. 4f). Increasing the pH induced a positive volumetric shift leading to an increment of the recorded P_t. Hence, the fiber probe's response for glucose detection depends on the pH of the solution. The measured P_t increased significantly starting from pH 6, which was due to swelling of the attached hydrogel sensor, caused by the increase in the anionic boronate ions in the hydrogel network. Decreasing the pH below 6 slightly shifted the output signal, indicating a tenuous growth in the anionic boronate ions, consistent with the previous studies (Zhang et al., 2013). Furthermore, the effect of temperature on the fiber probe's response was investigated within the range of 10–45 °C. Raising the solution's temperature induced shrinkage of the glucose-responsive hydrogel, enhancing the curvature of the imprinted microlenses, and consequently the output signal decreased. Within the temperature range of 20–35 °C, the fiber probe's signal slightly shifted, but the output signals considerably changed below 20 °C and above 35 °C. The output signal shifted by 2% when the temperature increased from 10 to 20 °C, 0.5% within 20–35 °C, and 3.6% when the temperature increased to 45 °C (Fig. 4g). The fiber's response to glucose should be calibrated at physiological conditions to avoid the temperature and pH interferences.

Silica fibers are not compatible with biological tissues to be implemented for *in vivo* sensing as they cause inflammation at the implanted sites and discomfort to patients. Therefore, a biocompatible hydrogel fiber was fabricated to replace the silica fiber. A biocompatible polymer, polyethylene glycol diacrylate (PEGDA) was utilized to fabricate hydrogel fibers because PEGDA hydrogel counters the adsorption of proteins such as fibrinogen, albumin, and fibronectin that

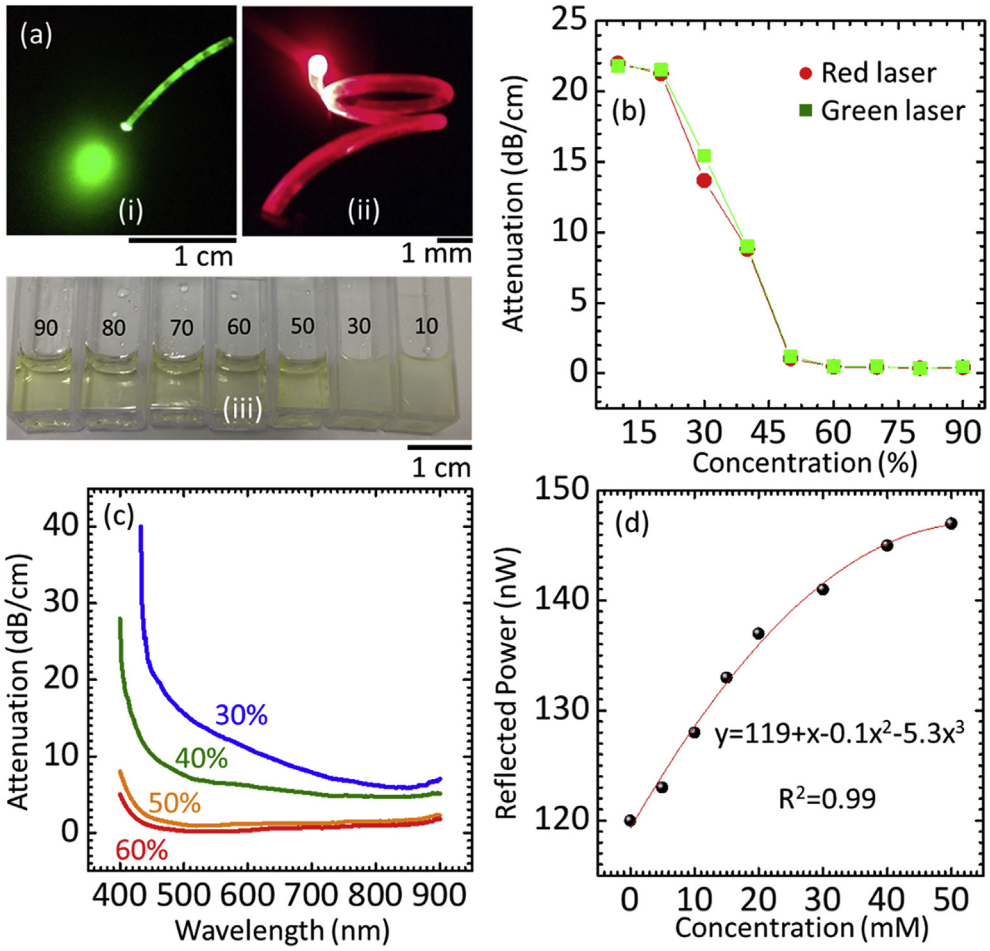

Fig. 5. Hydrogel optical fiber sensors. (a) Photographs of the functionalized hydrogel optical fiber and the PEGDA hydrogel cubes of various precursor concentrations. (b) The attenuation of green and red laser beams (532 and 650 nm) *versus* the precursor concentration (5–90 vol%). (c) The attenuation of the white light by the hydrogels of 1 cm cube side *versus* the precursor concentrations. (d) Testing the biocompatible functionalized fiber for glucose detection in the reflection configuration. The optical reflected power values were recorded by the power meter *versus* glucose concentrations. (For interpretation of the references to colour in this figure legend, the reader is referred to the Web version of this article.)

host the inflammatory cell interactions. Initially, polymerized PEGDA cubes of 1 cm side length were prepared at precursor concentrations of 5–90 vol% to determine the optimum concentrations for fabricating the hydrogel fiber (Fig. 5a). The hydrogel attenuation for monochromatic light (532 and 650 nm), and broadband white light were investigated. For monochromatic and white light, increasing the PEGDA concentration from 5 to 60 vol% considerably reduced the light attenuation, and above 60 vol% a slight change was detected (Fig. 5b and c). For monochromatic light, the attenuation was 22 dB cm^{-1} at the precursor concentration of 10 vol% and decreased to ~1 dB cm^{-1} when the precursor concentration reached 50 vol%. The attenuation decreased to ~0.4 dB cm^{-1} with increasing the precursor concentration to 90 vol%. These results confirmed that the optical properties of the PEGDA hydrogel depended on the precursor concentration which is consistent with the previous studies (Choi et al., 2015). The attenuation of the broadband white light measurements showed higher attenuation for short wavelengths besides the significant dependence of the attenuation on the precursor concentration. Considering the mechanical and optical properties, the hydrogel fiber was made of PEGDA precursor concentration of 60 vol%. The tip of the hydrogel optical fiber was functionalized with the glucose-responsive hydrogel as in the case of the silica fiber. The hydrogel fiber with a length of 5 cm and a diameter of 950 µm, was coupled with a broadband white light source and an optical power meter by the 2 × 1 coupler. The functionalized hydrogel fiber probe was interrogated for glucose sensing in the reflection mode and the readings were recorded after 15 min for each glucose concentration. The output signal increased by 17 nW within the glucose concentrations range of 0–20 mM and by 10 nW upon glucose concentration change from 20 to 50 mM, presenting analogous response to the functionalized silica fiber (Fig. 5d). The trend of the output signal was linear for the glucose concentration range of 0–20 mM and above this concentration the sensitivity decreased considerably. Notably, the sensitivity of the hydrogel fiber probe was less than the silica fiber which might be attributed to the higher light loss in the hydrogel fiber as compared to the silica fiber, and this matter can be tackled by cladding the hydrogel fiber with a low-refractive index material such as calcium alginate (Yetisen et al., 2017).

4. Conclusion

We have developed optical fiber probes for continuous glucose monitoring based on functionalizing the tips of a silica and a biocompatible hydrogel fibers. The functionalization process was carried out during the photopolymerization of the glucose-responsive hydrogel. The fabrication process of the fiber probe involved preparing the hydrogel, replicating the asymmetry microlens array, incorporating the 3-(acrylamido)phenylboronic acid, and attaching the hydrogel sensor to the fiber's tip, and was executed in 5 min. The facile and rapid fabrication process is one of the main advantages of the proposed fiber probe for glucose sensing. The PEGDA hydrogel was utilized to fabricate the biocompatible optical fiber that can potentially minimize the inflammation in the probe insertion site. The optical fiber's readout was simple, practical, and low cost as it did not require data processing or costly equipment. The output signals were recorded by either a smartphone or an optical power meter, utilizing broadband white light or monochromatic light sources for illuminating the probe. Glucose quantification tests were attained in the transmission and reflection configurations, and effect of pH and temperature on the fiber's response also was examined. The silica fiber probe was highly sensitive and selective for glucose than lactate within the physiological range as the

interference of lactate was trivial (~0.1%). The developed probe presented significant optical, mechanical, and practical advantages than their previous counterparts in terms of ease fabrication process, rapid response, and practical readouts. Therefore, the developed probe may find applications *in vivo* glucose monitoring systems at point-of-care and intensive care units. To realize broader applications, the proposed fiber probe can be functionalized with chelating agents and aptamers for continuously sensing a wide range of biomolecules such as proteins, DNA, and RNA in clinical samples.

Conflict of interests

The authors declare no competing financial interests.

Contributions

M.E. performed the experiments and wrote the manuscript. H.B. designed and led the study. M.U.H. and A.K.Y. made intellectual contributions and edited the article.

Appendix A. Supplementary data

Supplementary data to this article can be found online at https://doi.org/10.1016/j.bios.2019.05.002.

References

Bajgrowicz-Cieslak, M., et al., 2017. Optical glucose sensors based on hexagonally-packed 2.5-dimensional photonic concavities imprinted in phenylboronic acid functionalized hydrogel films. RSC Adv. 7, 53916–53924.

Boeckxstaens, G., Horowitz, M., Bermingham, H., Holloway, R., 1997. Physiological variations in blood glucose concentration affect oesophageal motility and sensation in normal subjects. Neuro Gastroenterol. Motil. 9, 239–246.

Cao, S., et al., 2018. Highly sensitive surface plasmon resonance biosensor based on a low-index polymer optical fiber. Optic Express 26, 3988–3994.

Choi, M., et al., 2013. Light-guiding hydrogels for cell-based sensing and optogenetic synthesis in vivo. Nat. Photon. 7, 987.

Choi, M., Humar, M., Kim, S., Yun, S.H., 2015. Step-index optical fiber made of biocompatible hydrogels. Adv. Mater. 27, 4081–4086.

Crofford, O., Genuth, S., Baker, L., 1987. Diabetes control and complications trial (DCCT): results of feasibility study. Diabetes Care 10, 1–19.

Doran, C.V., Chase, J.G., Shaw, G.M., Moorhead, K.T., Hudson, N.H., 2004. Automated insulin infusion trials in the intensive care unit. Diabetes Technol. Ther. 6, 155–165.

Elsherif, M., Hassan, M.U., Yetisen, A.K., Butt, H., 2018a. Glucose sensing with phenylboronic acid functionalized hydrogel-based optical diffusers. ACS Nano 12, 2283–2291. https://doi.org/10.1021/acsnano.7b07082.

Elsherif, M., Hassan, M.U., Yetisen, A.K., Butt, H., 2018b. Wearable contact lens biosensors for continuous glucose monitoring using smartphones. ACS Nano 12, 5452–5462.

Finney, S.J., Zekveld, C., Elia, A., Evans, T.W., 2003. Glucose control and mortality in critically ill patients. Jama 290, 2041–2047.

Haga, K.K., et al., 2011. The effect of tight glycaemic control, during and after cardiac surgery, on patient mortality and morbidity: a systematic review and meta-analysis. J. Cardiothorac. Surg. 6, 3.

Heller, A., Feldman, B., 2008. Electrochemical glucose sensors and their applications in diabetes management. Chem. Rev. 108, 2482–2505.

Heo, Y.J., Shibata, H., Okitsu, T., Kawanishi, T., Takeuchi, S., 2011. Long-term in vivo glucose monitoring using fluorescent hydrogel fibers. Proc. Natl. Acad. Sci. Unit. States Am. 108, 13399–13403.

Hisamitsu, I., Kataoka, K., Okano, T., Sakurai, Y., 1997. Glucose-responsive gel from phenylborate polymer and poly (vinyl alcohol): prompt response at physiological pH through the interaction of borate with amino group in the gel. Pharm. Res. (N. Y.) 14, 289–293.

James, T.D., Sandanayake, K.S., Shinkai, S., 1994. A glucose-selective molecular fluorescence sensor. Angew Chem. Int. Ed. Engl. 33, 2207–2209.

Kabilan, S., et al., 2005. Holographic glucose sensors. Biosens. Bioelectron. 20, 1602–1610.

Kondepati, V.R., Heise, H.M., 2007. Recent progress in analytical instrumentation for glycemic control in diabetic and critically ill patients. Anal. Bioanal. Chem. 388, 545.

Krinsley, J.S., Jones, R.L., 2006a. Cost analysis of intensive glycemic control in critically ill adult patients. CHEST Journal 129, 644–650.

Krinsley, J.S., Jones, R.L., 2006b. Cost analysis of intensive glycemic control in critically ill adult patients. Chest 129, 644–650.

Li, D., et al., 2015a. Solid-state sensors, actuators and microsystems (TRANSDUCERS). In: Transducers-2015 18th International Conference on. IEEE, pp. 1569–1572.

Li, D., et al., 2015b. Affinity based glucose measurement using fiber optic surface plasmon resonance sensor with surface modification by borate polymer. Sens. Actuators, B 213, 295–304.

Lin, T.-J., Chung, M.-F., 2009. Detection of cadmium by a fiber-optic biosensor based on localized surface plasmon resonance. Biosens. Bioelectron. 24, 1213–1218.

Montori, V.M., Bistrian, B.R., McMahon, M.M., 2002. Hyperglycemia in acutely ill patients. Jama 288, 2167–2169.

Rapsang, A.G., Shyam, D.C., 2014. Blood sugar control in the intensive care unit: time to relook. South. Afr. J. Anaesth. Analg. 20, 1–5. https://doi.org/10.1080/22201181.2015.959363.

Ruckh, T. T. & Clark, H. A. Vol. 86 1314-1323 (ACS Publications, 2013).

Singh, S., Gupta, B.D., 2013. Fabrication and characterization of a surface plasmon resonance based fiber optic sensor using gel entrapment technique for the detection of low glucose concentration. Sens. Actuators, B 177, 589–595.

Skyler, J.S., et al., 2009. Intensive glycemic control and the prevention of cardiovascular events: implications of the ACCORD, ADVANCE, and VA diabetes trials: a position statement of the American Diabetes Association and a scientific statement of the American College of Cardiology Foundation and the American Heart Association. Circulation 119, 351–357.

Srinivasan, M.P., et al., 2015. Factors associated with no apparent coronary artery disease in patients with type 2 diabetes mellitus for more than 10 years of duration: a case control study. Cardiovasc. Diabetol. 14, 146. https://doi.org/10.1186/s12933-015-0307-z.

Srivastava, S.K., Arora, V., Sapra, S., Gupta, B.D., 2012. Localized surface plasmon resonance-based fiber optic U-shaped biosensor for the detection of blood glucose. Plasmonics 7, 261–268.

The Action to Control Cardiovascular Risk in Diabetes Follow-On Eye Study, G, the Action to Control Cardiovascular Risk in Diabetes Follow-On Study, G, 2016. Persistent effects of intensive glycemic control on retinopathy in type 2 diabetes in the action to control cardiovascular risk in diabetes (ACCORD) follow-on study. Diabetes Care 39, 1089–1100.

Thomé-Duret, V., et al., 1996. Use of a subcutaneous glucose sensor to detect decreases in glucose concentration prior to observation in blood. Anal. Chem. 68, 3822–3826.

Thompson, C.L., Dunn, K.C., Menon, M.C., Kearns, L.E., Braithwaite, S.S., 2005. Hyperglycemia in the hospital. Diabetes Spectr. 18, 20–27.

Tierney, S., Falch, B.M.H., Hjelme, D.R., Stokke, B.T., 2009. Determination of glucose levels using a functionalized Hydrogel − optical fiber biosensor: toward continuous monitoring of blood glucose in vivo. Anal. Chem. 81, 3630–3636.

Umpierrez, G.E., et al., 2002. Hyperglycemia: an independent marker of in-hospital mortality in patients with undiagnosed diabetes. J. Clin. Endocrinol. Metab. 87, 978–982.

Vaddiraju, S., Burgess, D.J., Tomazos, I., Jain, F.C., Papadimitrakopoulos, F., 2010. Technologies for continuous glucose monitoring: current problems and future promises. Journal of diabetes science and technology 4, 1540–1562.

Van den Berghe, G., 2002. Insulin therapy in critical illness. International Diabetes Monitor 14, 1–6.

Van Den Berghe, G., et al., 2001. Intensive insulin therapy in critically ill patients. N. Engl. J. Med. 345, 1359–1367.

Van den Berghe, G., Wouters, P.J., Kesteloot, K., Hilleman, D.E., 2006. Analysis of healthcare resource utilization with intensive insulin therapy in critically ill patients. Crit. Care Med. 34, 612–616.

Veetil, J.V., Jin, S., Ye, K., 2010. A glucose sensor protein for continuous glucose monitoring. Biosens. Bioelectron. 26, 1650–1655.

Williams, L.S., et al., 2002. Effects of admission hyperglycemia on mortality and costs in acute ischemic stroke. Neurology 59, 67–71.

Yang, C., Chang, C., Lin, J., 2012. A comparison between venous and finger-prick blood sampling on values of blood glucose. International Proceedings of Chemical, Biological and Environmental Engineering 39, 206–210.

Yetisen, A.K., et al., 2017. Glucose-sensitive hydrogel optical fibers functionalized with phenylboronic acid. Adv. Mater. 29, 1606380–1606391.

Zhang, C., Losego, M.D., Braun, P.V., 2013. Hydrogel-based glucose sensors: effects of phenylboronic acid chemical structure on response. Chem. Mater. 25, 3239–3250.